

Published in final edited form as:

J Neurosci Methods. 2014 September 30; 0: 117–122. doi:10.1016/j.jneumeth.2014.05.025.

In-vivo testing of a non-invasive prototype device for the continuous monitoring of intracerebral hemorrhage

Madhuvanathi A. Kandadai, Ph.D.^{1,✦}, Joseph Korfhagen, Ph.D.^{2,✦}, Shauna Beiler, B.S.^{3,4}, Chris Beiler, B.S.^{3,4}, Kenneth Wagner, Ph.D.^{3,4}, Opeolu M. Adeoye, M.D.¹, and George J. Shaw, M.D., Ph.D.^{1,*}

¹Department of Emergency Medicine, 231 Albert Sabin Way, Suite 1358, University of Cincinnati, Cincinnati, Ohio 45267

²Department of Neuroscience, CARE/Crawley Building Suite E-870, University of Cincinnati, Cincinnati, Ohio 45267

³Department of Neurology, Stetson Building, 260 Stetson Street, Suite 2300, Cincinnati, OH 45267-0525

⁴Research Service, Veterans Affairs Medical Center, Cincinnati, Ohio 45220

Abstract

Background—Intracerebral hemorrhage (ICH) is a stroke subtype with the highest mortality rate. Hematoma expansion and re-bleeding post-ICH are common and exacerbate the initial cerebral insult. There is a need for continuous monitoring of the neurologic status of patients with an ICH injury.

New Method—A prototype device for non-invasive continuous monitoring of an ICH was developed and tested in-vivo using a porcine ICH model. The device consists of receiving and transmitting antennae in the 400–1000 MHz frequency range, placed directly in line with the site of the ICH. The device exploits the differences in the dielectric properties and geometry of tissue media of a healthy brain and a brain with an ICH injury. The power received by the receiving antenna is measured and the percent change in power received immediately after infusion of blood and 30 minutes after the infusion, allowing for the blood to clot, is calculated.

Results—An increase in the received power in the presence of an ICH is observed at 400 MHz, consistent with previous in-vitro studies. Frequency sweep experiments show a maximum percent change in received power in the 750–1000 MHz frequency range.

© 2014 Elsevier B.V. All rights reserved.

*Corresponding Author: Madhuvanathi A. Kandadai, Ph.D., Department of Emergency Medicine, 231 Albert Sabin Way, Cincinnati, OH 45267-0769, United States. Tel.: +1 513 558 5293; fax: +1 513 558 5791. kandadmi@ucmail.uc.edu.

✦These authors contributed equally to the work

Disclosures

GJS and OA are co-inventors on the patent application (#10738-186) which covers some of the technology discussed in this work.

Publisher's Disclaimer: This is a PDF file of an unedited manuscript that has been accepted for publication. As a service to our customers we are providing this early version of the manuscript. The manuscript will undergo copyediting, typesetting, and review of the resulting proof before it is published in its final citable form. Please note that during the production process errors may be discovered which could affect the content, and all legal disclaimers that apply to the journal pertain.

Comparison with existing methods—Currently, CT, MRI and catheter angiography (CA) are the main clinical neuroimaging modalities. However, these techniques require specialized equipment and personnel, substantial time, and patient- transportation to a radiology suite to obtain results. Moreover, CA is invasive and uses intra-venous dye or vascular catheters to accomplish the imaging.

Conclusions—The device has the potential to significantly improve neurologic care in the critically ill brain-injured patient.

INTRODUCTION

Spontaneous intra-cerebral hemorrhage (ICH) accounts for over 2 million strokes per year with a mortality rate of more than 50% at one year.^{1–5} Early neurologic deterioration (drop in Glasgow Coma Scale or GCS of 2 points or more) is observed in more than 20% of ICH patients between pre-hospital evaluation by the emergency medical service personnel and neuroimaging in the Emergency Department (ED).⁶ A mortality rate of more than 75% is observed in this group of patients. Moreover, hematoma expansion of greater than one-third the initial volume is seen in the follow-up computed tomography (CT) of 28–38 % of patients who undergo initial CT assessment within three hours of ICH onset.^{7–9} Aggressive medical care to curb early neurological deficit due to hematoma expansion is crucial in improving patient outcomes.⁶

In the ED, CT is the recommended neuroimaging modality for the identification and subsequent evaluation of an ICH. However, patients may be comatose, sedated and/or paralyzed for intubation. Allowing injured patients to wake up for a neurologic exam while on a ventilator or moving the patient to the radiology suite for imaging can be uncomfortable and potentially dangerous. Real-time monitoring of the rate and size of hematoma expansion has been suggested as more beneficial in ICH management and treatment than serial imaging over time.¹⁰ Hence, there is a need for a non-invasive, portable device for the continuous monitoring of ICH and hematoma expansion.

In a previous publication, we presented proof-of-concept data for an electromagnetic (EM) radiofrequency (RF) based prototype device for ICH continuous monitoring in-vitro using a brain tissue simulating gel model.¹¹ Our results showed a linear dependence of the increase in received power on the size of the blood pool in the ICH brain gel model. In this paper, we present results from in-vivo experiments on a porcine ICH model using the prototype device at a frequency of 400 MHz, and results from frequency sweep experiments in the 400–1000 MHz range.

METHODS

Porcine ICH model

Animal Preparation—After appropriate IACUC review and approval of the protocol, a porcine frontal lobar ICH model developed by Wagner et. al. was used.^{12, 13} Juvenile pigs were purchased at about 9 weeks of age; a typical weight was 20 kg. Pigs were anesthetized using intramuscularly delivered ketamine (25–30 mg/kg) followed by intravenously administered pentobarbital (35 mg/kg) to achieve deep anesthesia. Anesthesia was

maintained throughout the experiment by intravenous pentobarbital infusion (10 mg/kg/hour). Exclusion criteria include coagulation of blood in the catheter prior to infusion into the pig head, leakage from the tubing into other parts of the pig head leading to poor control over the amount and location of blood in the brain, or unintended changes in antennae position due to user-error over the course of the experiments causing misalignment of antennae with predicted ICH location.

Surgical Preparation, Physiological Monitoring, and Blood Infusion—All surgical procedures were performed using aseptic techniques. Pigs were mechanically ventilated (supplemented with 1 L/minute oxygen) and femoral arteries catheterized for continuous blood pressure readings and for blood sampling to determine blood gas and pH. Femoral veins were catheterized for infusion of saline and pharmacological agents. The animals' core temperature was measured with a rectal thermistor probe and maintained at $38.5 \pm 0.5^\circ\text{C}$ during the entire procedure.

The skin on top of the head was incised and spread to expose the skull and an 18-gauge catheter was placed in the right frontal cortex. Experimental ICH was produced by a 15-minute infusion of autologous blood (3.0 mL obtained from the femoral arterial line) through the catheter into the centrum semiovale of the right frontal cerebral white matter.

Brain Tissue Fixation, Coronal Sectioning, and Photography—At 3 hours after blood infusion and completion of RF measurements, pig brains were frozen *in-situ* with liquid nitrogen. The frozen heads were cut into 7-mm thick coronal sections using a bandsaw for anatomic imaging and measurement of the ICH and hematoma. Both sides of the coronal sections containing hematomas were photographed next to a millimeter scale ruler. Areas of experimental ICH were then determined using computer-assisted morphometry on workstations equipped with ImageTool (University of Texas Health Sciences Center, San Antonio, TX) and corrected for image size based on the millimeter ruler. The areas from both sides of each slice were averaged and the values multiplied by its thickness to calculate slice volumes. Volumes of slices containing hematomas were summed to calculate the total hematoma for each brain.

Device Setup

400 MHz Experiments—After the pig was anesthetized, its body and head were raised such that the upper eyelids were 26–28 cm in height from the table. The transmitting antenna (PCB Log Periodic WA5VJB, Ramsey Electronics, Victor, NY) was placed horizontally on the left side of the head (Figure 1). The receiving antenna (SATCOM UL-3001-340-CF portable UHF, Myers Engineering International, Inc., Margate, FL) was placed horizontally on the right side of the head. The antennae were placed 15 cm apart and aligned collinearly with the upper eyelids, an external landmark collinear with the approximate location of the hematoma in the frontal white matter. A dot corresponding to the center of the transmitting antenna was drawn on the head in order to determine if the antennae were collinear with the clot after the head was cut. A signal generator (HP8657B, Hewlett Packard, Palo Alto, CA) was used to generate a signal at a frequency of 400 MHz and amplitude of 1.5V into an RF Amplifier (ENI607L, ENI, Rochester, NY). The amplifier

output was connected to the transmitting antenna. Power received by the receiving antenna was measured by a spectrum analyzer (HP8560E, Hewlett Packard, Palo Alto, CA). Spectrum power data was collected manually over a bandwidth of 10 MHz with the center frequency at 400MHz. Forty measurements were made over a two-minute period for three different experiments: after catheter insertion but before blood infusion ($P_{R(\text{CONTROL})}$), immediately after blood infusion ($P_{R(\text{ICH}(0))}$), and 30 minutes after the initial ICH measurements ($P_{R(\text{ICH}(30))}$) to give the blood time to clot. These measurements were averaged and a standard deviation was calculated for each experiment. From this data, the percentage change () was calculated as shown below:

$$\Delta_{\text{ICH}(0)} = (P_{R(\text{ICH}(0))} - P_{R(\text{CONTROL})}) / P_{R(\text{CONTROL})} \quad (1)$$

$$\Delta_{\text{ICH}(30)} = (P_{R(\text{ICH}(30))} - P_{R(\text{CONTROL})}) / P_{R(\text{CONTROL})} \quad (2)$$

Frequency Sweep Experiment—For the frequency sweep experiments, the transmitting and receiving antennae were identical (PCB Log Periodic WA5VJB, Ramsey Electronics, Victor, NY). Two log-periodic broadband antennae were used because their directivity allowed for a higher signal-to-noise ratio in the region of interest (the location of the hematoma), compared to the omnidirectional receiving antenna used previously. They were placed at the same height and collinear with the same anatomical locations as the 400 MHz experiments, but were vertically aligned (Figure 2). The antennae were vertically polarized to cover a larger cross-sectional area of the brain and to reduce sensitivity to antennae alignment with the location of the hematoma. The distance between the antennae varied between 11–13 cm to accommodate variations in pig biparietal diameter. The same signal generator, amplifier, and spectrum analyzer were used. The remainder of the experimental set-up was the same as the 400 MHz experiments.

A MATLAB (v.7.10.0.499, Mathworks Inc., Natick, MA) program was written to communicate with the signal generator and spectrum analyzer using a computer. The program would complete a frequency sweep from 400 to 1000 MHz at 50 MHz intervals. Twenty measurements over a 30-second period were taken for each frequency for the same control, ICH(0), and ICH(30) parameters. The value was calculated for ICH(0) and ICH(30).

Antennae Stability Experiments—The power received by the receiving antenna was monitored over a period of 90 minutes in the 400–1000 MHz frequency range in order to ensure that the variability in experimental readings were not a result of intrinsic fluctuations or drift in antennae radiations over time. These experiments were done without a pig present between the antennae. For three different experiments, coefficient of variation (c_v) was calculated. Due to the variability of the antennae, c_v was used to determine the normal drift of the antennae over time. Average percent drift could then be calculated by averaging the c_v values for each drift experiment.

Statistical Analysis

SigmaPlot 11.0 statistical software (San Jose, California, USA) was used for statistical analysis. Means and standard deviations of the data were calculated as needed. Student's paired t-test was used to determine the statistical significance of and a $p < 0.05$ was considered significant.

RESULTS

400 MHz experiments

The $ICH(0)$ and $ICH(30)$ measurements are shown in Figure 3. Overall, there was an increase in P_R after blood infusion, corresponding to an average $ICH(0)$ value of $14 \pm 6\%$ ($p < 0.05$). In 4 out of the 5 pigs studied, the increase in the $ICH(0)$ values were sustained even after 30 minutes ($ICH(30)$ measurements) ($p < 0.05$). However, no significant increase in the average $ICH(30)$ value ($13 \pm 11\%$) compared to $ICH(0)$ values was observed. The average volume of the retracted clots for these experiments determined from the frozen slices was 1.1 ± 0.3 cc.

Frequency sweep experiments

Figure 4 shows the average P_R values for a representative experiment. As shown in Figure 5, a statistically significant increase in $ICH(0)$ and $ICH(30)$ was observed for the 750–1000 MHz frequency range. A significant increase in $ICH(30)$ was also observed for 500, 550, and 700 MHz frequencies. There was not a significant increase between any of the $ICH(0)$ and $ICH(30)$ measurements, but a trend toward significance was observed for 750–1000 MHz. As visualized by the large standard deviations, pig-to-pig variability was observed in the frequency sweep experiments, similar to the 400 MHz experiments.

Antenna stability experiment

Three drift experiments were completed with the average percent drift values ranging from 1.1–2.4% (Figure 5).

DISCUSSION

In summary, we have developed a non-invasive prototype device for the continuous monitoring of ICH and tested it using a porcine ICH model in-vivo. The increase in the received power after ICH was induced in the pig brain was consistent with our previously published in-vitro data at 400 MHz. A greater increase in received power was observed at higher frequencies in the 750–1000 MHz range. This technique may be useful in the future to monitor changes in the intra-cranial region of patients suffering from ICH, traumatic brain injury, or other hemorrhagic brain injuries.

Korfhagen *et. al.* used this technique in *in vitro* studies on an ICH gel model using the prototype device also used in this work.¹¹ Their studies showed an increase in received power upon introduction of citrated human blood in the gel model. Overall, the significant increase ($p < 0.05$) in received power after infusion of blood in this *in vivo* work was consistent with the previously published in *vitro* results. However, a higher percent increase

(14%) in received power was observed *in-vivo* than for previous *in vitro* experiments of the same volume (2–3% increase). Numerous factors not present with *in vitro* experimentation could attribute to this larger increase. Changes in the geometry of the brain in response to the ICH such as gyri shift and a decrease in ventricular space, or the physiologic response to the brain injury could have played a role. Furthermore, in the *in vitro* experiments, the blood cavity was always placed in the center of a brain-mimicking gelatin, which was centered between the antennae. Infusion in the right frontal lobe of the pig resulted in the ICH being located closer to the receiving antennae. The distance of the ICH from the transmitting antennae may also affect the signal. Moreover, autologous blood was used for the *in-vivo* experiments, whereas citrated human blood was used in the *in-vitro* work, potentially modifying the effective dielectric constant of the in-vitro experiments.

After allowing the blood to clot, a slight increase in received power was observed for 4 of the 5 pigs. This may have been due to the changing geometry of the hematoma as the blood clots. For pig 5, the decrease seen with the ICH(30) measurement may have been due to poor alignment of the antennae with the location of the clot. After viewing frozen brain slices, it was determined that the antennae were not collinear with the clot based on the location of the clot with respect to the eyes. In addition, for this pig, blood was found in the subarachnoid space (Figure 6). This finding did not occur in the other pigs. It may have been due to the pressure gradient created by removing the tubing after blood infusion which caused backflow along the catheter into the subarachnoid space. Considering the clot was 25% smaller than average clot size for these experiments, and not collinear with the antennae, it is difficult to determine the amount of blood collinear with the antennae during each measurement. Finally, the diameter of the head for this pig was larger than the others, so more biological material was present for the RF signal to traverse than for previous experiments. Taking all of these observations into account, even though there was a clot present in the brain, excluding pig 5 data would result in average ICH(0) and ICH(30) values of $14.2 \pm 7\%$ and $16.9 \pm 7\%$ at 400 MHz using this antennae configuration, respectively. No significant difference between average ICH(0) and ICH(30) is found even with excluding pig 5 data.

A larger ICH(0) and ICH(30) was observed for higher frequencies (750–1000 MHz). Also, standard deviations (pig-to-pig variability) were smaller at these frequencies. The highest ICH and Clot values observed at 850 MHz. Although statistically significant, the ICH(0) and ICH(30) values at 850 MHz may be due to the lower received power at this frequency, and hence, may not be indicative of a greater sensitivity to ICH than the other frequencies (500, 550, 700 and the 750–1000 MHz frequency range) with statistically significant ICH(0) and ICH(30) values. At 400 MHz, much smaller increases were seen compared to previous data. This could have been due to the change in antennae configuration, which causes the beam profile emitted by the antennae to change, or the change in distance between the antennae to accommodate differing pig head sizes. For these five experiments, the variable distance (11–13 cm) between the antennae was not expected to have a large effect on received power because a 10% change in distance yielded a 3% difference in received power in previous experiments.¹¹ The antennae were placed as close to the head as possible without making contact to maintain a consistent distance between the transmitting antenna

and the location of the clot between experiments. This is an optimal characteristic from a design perspective if this device will eventually be used on humans with varying head diameters.

For the majority of the frequencies studied using this configuration, the average $ICH(0)$ was greater than 3%, which is larger than the average percent drift for these frequencies. Therefore, drift of the antennae did not affect the $ICH(0)$ and $ICH(30)$ results. However, the average difference seen between $ICH(0)$ and $ICH(30)$ could have been due to drift alone during the experiment. Antennae stability will be important to consider for future prototype design because the setup used in these experiments was sensitive to the day-to-day changes in the environment causing large baseline variability. However, once in the environment, the antennae remained stable for long periods of time, suggesting that factors such as external electrical interference, appliance noise, and day-to-day variations in room temperature did not significantly affect the received power measurements over time. Another limitation of this work was that accurate measurements could be made only with the position of the head unchanged with respect to the antennae. Future device designs will address this limitation. However, previous in-vitro measurements using this device show that a change in the distance between the antennae of about 15 mm was required to observe a 3% change in received power.¹¹

There were numerous advantages to using this porcine ICH model. Previously, *in vitro*, the device could detect as little as 1 mL of blood. Due to the size of the antennae, a vertebrate animal ICH model large enough to infuse at least 1 mL of blood was required. This model has a 3 mL infusion, a comparable amount of blood to previous *in vitro* experiments. During *in vitro* experiments, the blood could be placed collinearly with the antennae. With the *in vivo* setup such that the antennae are aligned collinearly with the predicted location of the ICH, the exact location of the ICH could vary slightly, and therefore, the ICH would not be collinear with the antennae if an insufficient amount of blood was infused. A 3-mL infusion allowed for a large enough area such that the antennae were collinear with the ICH for all but one of the experiments. Finally, the bone-thickness is comparable to a human, and the pig brain has gyri and ventricles, which could affect the RF signal.¹⁴

While utilizing RF antennae to monitor for changes resulting from an ICH is a promising technology, other technologies such as near infrared spectroscopy (NIRS) and electrical impedance tomography (EIT) have also shown great progress in assessing for ICH. A device has been developed for detecting ICH using near-infrared absorption by Infrascan, Inc. (Philadelphia, Pennsylvania, USA). Numerous clinical studies have been completed using this device. Robertson et al. recently showed that their device can accurately detect 88% of hematomas that are within 2.5 cm of the surface of the brain.¹⁵ While this is a significant development for the detection of superficial hematomas, sensitivity to deep cerebral hemorrhages is much lower using this technique (68%). Regardless, this is the best current technique for non-invasively monitoring ICH besides CT or MRI. The only major limitation of this technique is that the presence of hair can limit the efficacy of the technique.

EIT uses electrodes on the scalp to monitor for changes in impedance across the brain.^{16, 17} Two relevant animal studies have looked at changes in impedance due to inducing

hemorrhage in an *in vivo* piglet model¹⁶ and an *in vivo* rabbit model.¹⁷ Both of these studies found that impedance tomography could detect changes in impedance due to ICH at very early stages. The major limitation of this technique is the requirement that the electrodes must be in good electrical contact with the scalp, which may be difficult to accomplish in emergency situations. Also, detecting ICH is based on a relative change in impedance over time.

Acknowledgments

The authors gratefully acknowledge the support of the Point-Of-Care Center for Emergency Neuro-Technologies (POCCENT) grant program as funded through NIBIB/NIH, and the University of Cincinnati Technology Commercialization Accelerator funding. The authors also would like to thank the Department of Emergency Medicine at the University of Cincinnati for equipment funding. The porcine studies were supported in part by Merit Review funds from the Department of Veterans Affairs.

References

1. Qureshi AI, Mendelow AD, Hanley DF. Intracerebral haemorrhage. *Lancet*. 2009; 373:1632–1644. [PubMed: 19427958]
2. Hansen BM, Nilsson OG, Anderson H, Norrving B, Säveland H, Lindgren A. Long term (13 years) prognosis after primary intracerebral haemorrhage: A prospective population based study of long term mortality, prognostic factors and causes of death. *Journal of Neurology, Neurosurgery & Psychiatry*. 2013; 84:1150–1155.
3. Flaherty ML, Haverbusch M, Sekar P, Kissela B, Kleindorfer D, Moomaw CJ, Sauerbeck L, Schneider A, Broderick JP, Woo D. Long-term mortality after intracerebral hemorrhage. *Neurology*. 2006; 66:1182–1186. [PubMed: 16636234]
4. Labovitz DL, Halim A, Boden-Albala B, Hauser WA, Sacco RL. The incidence of deep and lobar intracerebral hemorrhage in whites, blacks, and hispanics. *Neurology*. 2005; 65:518–522. [PubMed: 16116109]
5. Sudlow CL, Warlow CP. Comparable studies of the incidence of stroke and its pathological types: Results from an international collaboration. *International stroke incidence collaboration*. *Stroke*. 1997; 28:491–499. [PubMed: 9056601]
6. Morgenstern LB, Hemphill JC, Anderson C, Becker K, Broderick JP, Connolly ES, Greenberg SM, Huang JN, Macdonald RL, Messé SR, Mitchell PH, Selim M, Tamargo RJ. On behalf of the american heart association stroke council on cardiovascular nursing. Guidelines for the management of spontaneous intracerebral hemorrhage: A guideline for healthcare professionals from the american heart association/american stroke association. *Stroke*. 2010; 41:2108–2129. [PubMed: 20651276]
7. Davis SM, Broderick J, Hennerici M, Brun NC, Diringer MN, Mayer SA, Begtrup K, Steiner T. Recombinant activated factor vii intracerebral hemorrhage trial investigators. Hematoma growth is a determinant of mortality and poor outcome after intracerebral hemorrhage. *Neurology*. 2006; 66:1175–1181. [PubMed: 16636233]
8. Broderick JP, Duldner JE, Tomsick T, Huster G. Volume of intracerebral hemorrhage. A powerful and easy-to-use predictor of 30-day mortality. *Stroke*. 1993; 24:987–993. [PubMed: 8322400]
9. Brott T, Broderick J, Kothari R, Barsan W, Tomsick T, Sauerbeck L, Spilker J, Duldner J, Khoury J. Early hemorrhage growth in patients with intracerebral hemorrhage. *Stroke*. 1997; 28:1–5. [PubMed: 8996478]
10. Ninds ich workshop participants. Priorities for clinical research in intracerebral hemorrhage: Report from a national institute of neurological disorders and stroke workshop. *Stroke*. 2005; 36:E23–E41. [PubMed: 15692109]
11. Korfhagen JJ, Kandadai MA, AOA, Clark J, Shaw GJ. A prototype device for non-invasive continuous monitoring of intracerebral hemorrhage. *Journal of neuroscience methods*. 2012;9. [PubMed: 22068031]

12. Wagner KR, Xi G, Hua Y, Kleinholz M, de Courten-Myers GM, Myers RE, Broderick JP, Brott TG. Lobar intracerebral hemorrhage model in pigs: Rapid edema development in perihematomal white matter. *Stroke*. 1996; 27:490–497. [PubMed: 8610319]
13. Wagner KR, Xi G, Hua Y, Zuccarello M, de Courten-Myers GM, Broderick JP, Brott TG. Ultra-early clot aspiration after lysis with tissue plasminogen activator in a porcine model of intracerebral hemorrhage: Edema reduction and blood-brain barrier protection. *J Neurosurg*. 1999; 90:491–498. [PubMed: 10067918]
14. Sun Z, Lee E, Herring SW. Cranial sutures and bones: Growth and fusion in relation to masticatory strain. *Anat Rec A Discov Mol Cell Evol Biol*. 2004:276.
15. Robertson CS, Zager EL, Narayan RK, Handly N, Sharma A, Hanley DF, Garza H, Maloney-Wilensky E, Plaum JM, Koenig CH, Johnson A, Morgan T. Clinical evaluation of a portable near-infrared device for detection of traumatic intracranial hematomas. *Journal of Neurotrauma*. 2010; 27:1597–1604. [PubMed: 20568959]
16. Xu CH, Wang L, Shi XT, You FS, Fu F, Liu RG, Dai M, Zhao ZW, Gao GD, Dong XZ. Real-time imaging and detection of intracranial hemorrhage by electrical impedance tomography in a piglet model. *Journal of International Medical Research*. 2010; 38:1596–1604. [PubMed: 21309473]
17. Chen, C.; Fu, F.; Li, B.; Liu, W.; Xu, S.; Tao, F.; Shi, X.; Yang, L.; Fei, Z.; Dong, X. Experimental study of detection of brain tissue with electrical impedance tomography after cerebral ischemic. In: Long, M., editor. *World congress on medical physics and biomedical engineering may*; 26–31, 2012; beijing, china. Berlin Heidelberg: Springer; 2013. p. 807-810.

Highlights

A device for continuous monitoring of an intracerebral hemorrhage (ICH) was developed.

The non-invasive device was tested in-vivo using a porcine ICH model.

The device consists of transmitting and receiving antennae placed in line with the site of the ICH.

The power received by the receiving antenna was measured before and after ICH injury.

The increase in the received power after ICH injury was highest in the 750–1000 MHz frequency range.

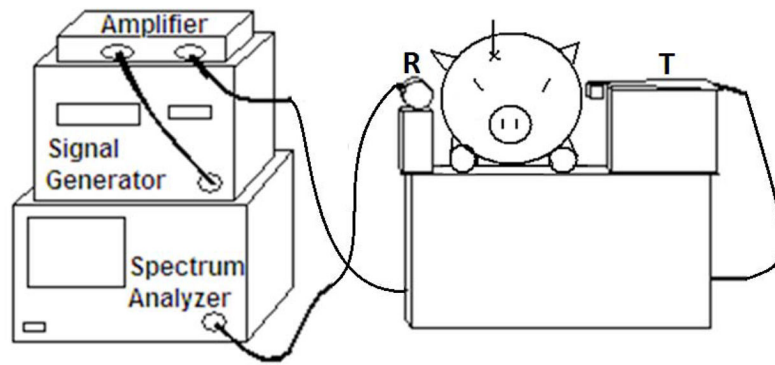


Figure 1. Schematic of the 400 MHz experimental setup. The transmitting antenna is on the left side of the pig head and the receiving antenna is on the right.

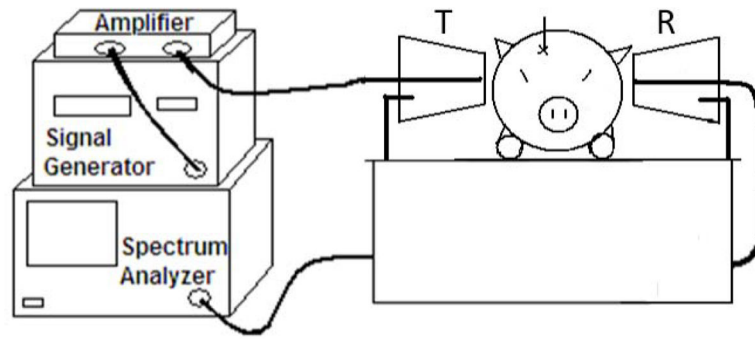


Figure 2. Schematic of the frequency sweep experimental setup. The transmitting antenna is on the right side of the head and the receiving antenna is on the left.

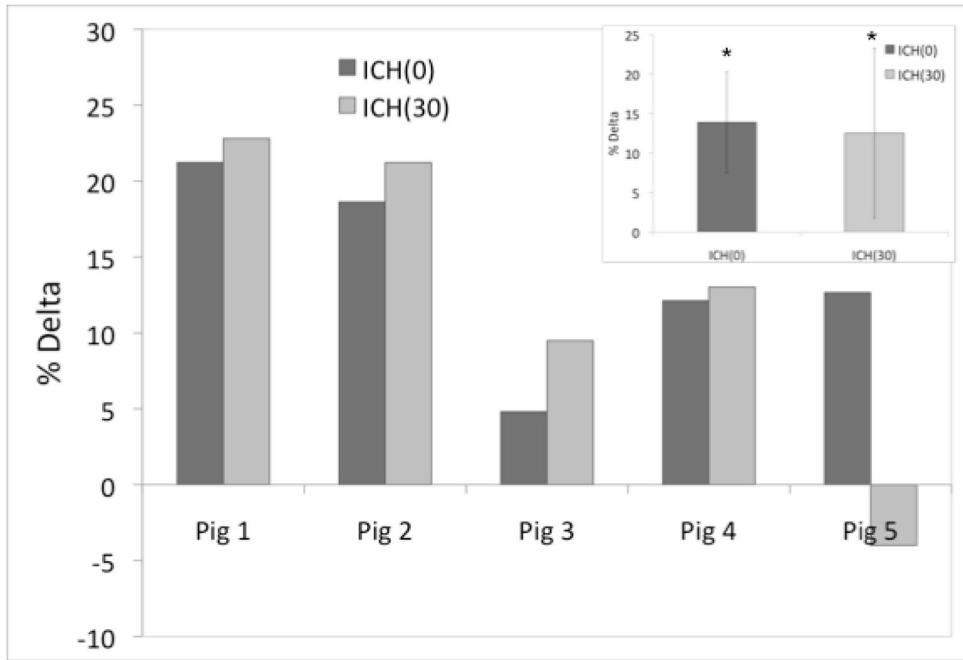


Figure 3. The percent delta values obtained using the 400 MHz experiment setup, with the statistically significant average percent delta values shown in the insert.

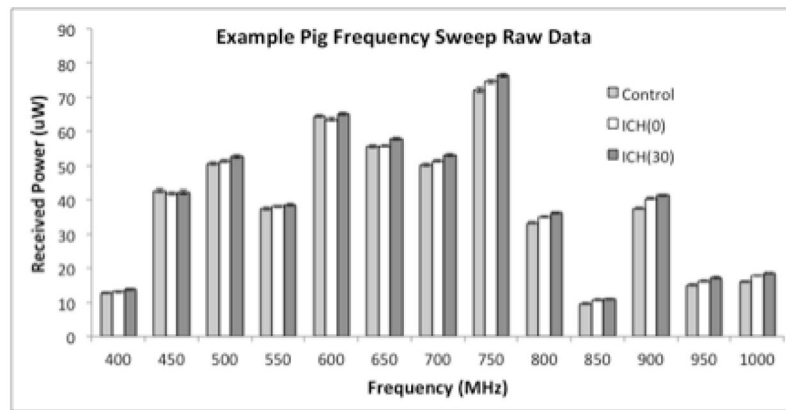


Figure 4. Typical P_R values for each condition in the frequency sweep experiment showing frequency variability.

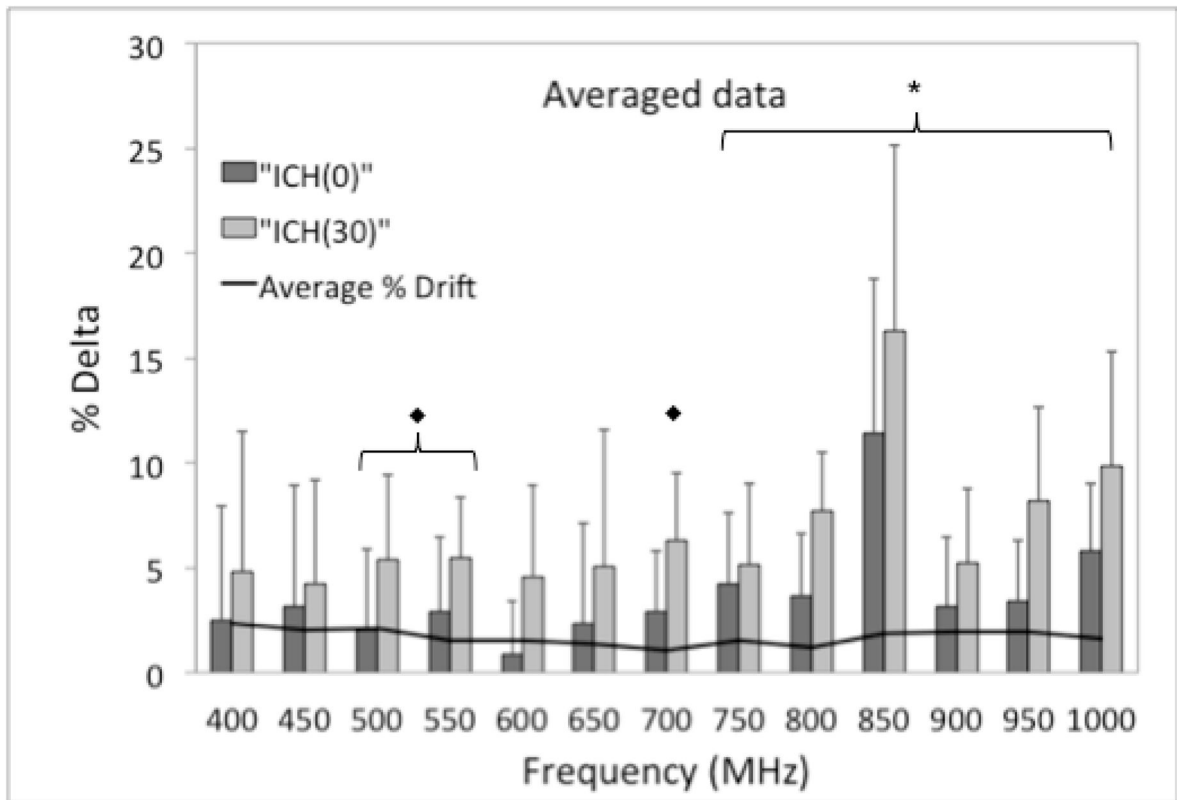


Figure 5.

Average % Δ for frequency sweep experiments (N=5) showing the effect of ICH and subsequent clotting in the brain. The solid line represents the average % Drift (N=3) of the antennae. The significance marker "◆" represents the frequencies at which a statistically significant increase in Δ ICH(30) was observed (500, 550, and 700 MHz). The significance marker "X" represents the frequencies at which statistically significant increases in both Δ ICH(0) and Δ ICH(30) were observed (750–1000 MHz).

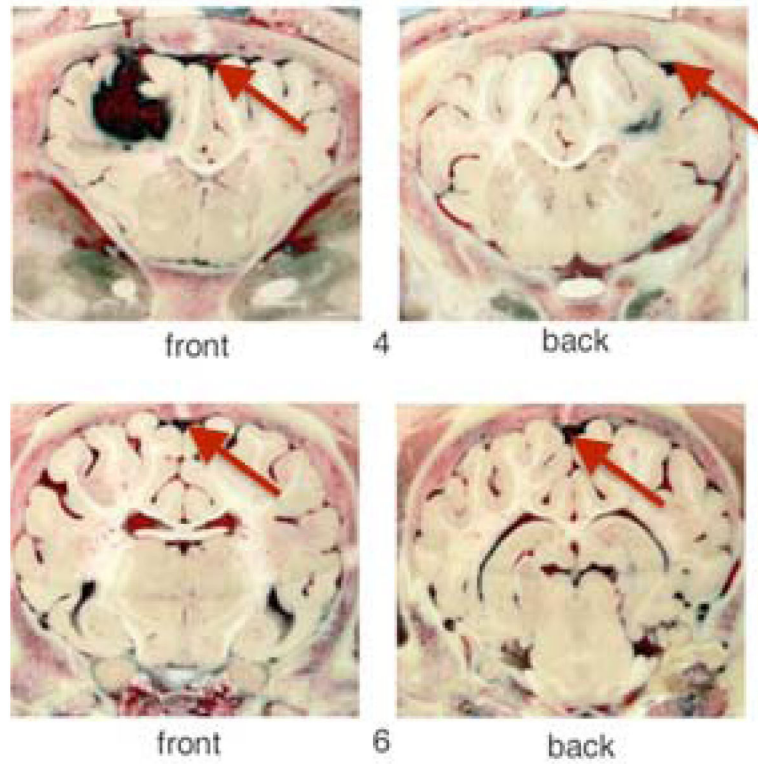


Figure 6. Photographs of frozen coronal brain slices from pig 5 showing clot in the frontal lobe and the presence of blood in the subarachnoid space (red arrows) which may have affected $P_R(\text{ICH}(0))$ and $P_R(\text{ICH}(30))$ measurements.